Desalination and Water Treatment
www.deswater.com

doi: 10.5004/dwt.2022.28097

252 (2022) 18–27
March

Performance analysis of a solar seawater desalination using an ultra-black nylon flocking material

Chao Miao[a,*], Jianbo Ren[a], Min Wang[a], Chungang Xie[a], Lingpin Zhang[a], Qiang Li[a], Hui Zhang[b]

[a]*The Institute of Seawater Desalination and Multipurpose Utilization, MNR (Tianjin), No. 55, Hanghai Road, Nankai District, Tianjin 300192, China, Tel. +86 22 877898150; emails: miao-chao@hotmail.com (C. Miao), 13752797531@163.com (J. Ren), wangmira@outlook.com (M. Wang), acds120@163.com (C. Xie), zhanglingpin@163.com (L. Zhang), 373692041@qq.com (Q. Li)*
[b]*National Center for Nanoscience and Technology, No. 11, ZhongGuanCun BeiYiTiao, Beijing 100190, China, Tel. +86 10 82545579; email: zhangh@nanoctr.cn*

Received 1 July 2021; Accepted 24 December 2021

ABSTRACT

Solar-driven seawater desalination has emerged as a promising strategy to solve the global water crisis with green energy. In this paper, an ultra-black nylon flocking photothermal material was developed and applied as a solar evaporator. The theoretical analysis of high-efficiency interfacial evaporation was introduced. The performance of the evaporator in terms of evaporation rate and salt resistance was evaluated through the experimental verification method. With the introduction of the ultra-black nylon flocking material, the evaporation efficiency increased by 76.06% for seawater desalination. In the long-term stability test, the average evaporation rate was above 1.20 kg/m^2 h. Evaporation and condensation experiments were further carried out using a small solar distiller. The results showed that installing ultra-black nylon flocking material in traditional disc-type solar distiller could increase the water production from the original 2.8 to 7.76 kg/m^2 d. Without the condensation chamber, the amount of vapor evaporating out to the ambient environment was up to 10.24 kg/m^2 d. Thus, facilitating the steam condensation while improving the evaporation efficiency is of great significance to the broad application of solar desalination.

Keywords: Seawater desalination; Solar energy; High-efficiency interfacial evaporation; Experiment verification

1. Introduction

Solar-driven seawater desalination is a technique that produces freshwater by harvesting solar thermal energy to heat the seawater for evaporation and condensation. However, it had several drawbacks such as low operating temperature, low water production, insufficient low solar energy utilization, and high equipment cost, which have greatly limited its practical application. Under the best operating conditions, the thermal efficiency is only 35%, and the water production per unit area is 3 ~ 4 kg/m^2 d [1,2]. The reasons lie in the facts that the heat capacity of the seawater to be evaporated is too large, and the photothermal conversion efficiency is low, which weaken the driving force for evaporation. Efforts have been devoted to improving the performance of the solar distiller, which include adding dyes [3], charcoal [4], sponges [5], calcium stones, black granite gravel and pebbles [6], etc. into the seawater to reduce the heat capacity of the seawater in the device; painting the trays with manganese oxide nanoparticles [7],

* Corresponding author.

SiO_2/TiO_2 coatings [8,9] to improve heat transfer characteristics; adding phase change material to store excess solar heat and extend operating time [10–15]; designing a multistage stacked tray [16] to recover the condensation latent heat of steam, etc. Still, the water production of the solar distiller is far from enough. Active solar desalination system strengthens convection heat transfer, but it normally requires an ancillary equipment to raise the operating temperature to facilitate the internal heat and mass transfer process. The common ancillary equipment includes the external collector [17], internal or external condenser [18], rotating disc or drum [19–24], fan [25,26], and mirror [27], etc. With the introduction of ancillary equipment, the cost of the system is increased, the operation stability is decreased, and external power equipment is often required. Therefore, to simultaneously increase the solar radiation absorption rate and the solar photothermal conversion efficiency is essential for improving the water production per unit area.

In recent years, researchers have successively developed a series of highly efficient photothermal materials for solar desalination. These photothermal materials can be divided into four types, including metal plasmonic materials, carbon-based materials, polymer composite materials and biological composite materials.

1.1. Metal plasmonic materials

Metal plasmonic materials with the strong absorption of solar light, show the great potential for the utilization of solar energy. For efficient photothermal conversion from a wider solar spectrum, flexible thin-film black gold membranes were prepared employing adiabatic plasmonic nanofocusing technology [28], which had multiscale structures of varied metallic nanoscale gaps (0–200 nm) as well as microscale funnel structures. The adiabatic nanofocusing of self-aggregated metallic nanowire bundle arrays produced average absorption rate of 91% at 400–2,500 nm and the microscale funnel structures led to average reflection of 7% at 2,500–17,000 nm. This system enabled solar thermal conversion efficiency up to 57% at 20 kW/m^2. The three-dimensional self-assembled aluminum nanoparticles have been developed by Zhu Jia's group of Nanjing University. The average absorption rate was as high as 96% at 400–2,500 nm spectral range [29].

1.2. Carbon based materials

Carbon based photothermal conversion materials are promising candidates for solar thermal-related application. MIT uses graphite sheets and foamed carbon to form a porous and insulating material. When sunlight shines on the surface of the material, it forms a hot spot in the graphite, which can guide water through these holes and form water steam [30]. Yang et al. [31] developed a graphene-based independent solar energy converter for desalination and purification. It consists of a prefabricated 3D cross-connected honeycomb graphite foam material, which can be used to obtain fresh water from seawater and sewage under environmental conditions. Peking University recently announced a graphene foam material with a multi-level structure, with a photothermal conversion efficiency of 93.4% [32]. The State University of New York in the United States reported a black paper-based light-absorbing material with an absorption rate of 98% in the range of 250–2,500 nm, and the thermal conversion efficiency of its solar distillation experimental device under a solar radiation intensity reached 88% [33]. A simple method toward fabricating graphene aerogel (GA) from graphene oxides only by photoreduction was reported, which was for the first time used to harvest solar energy. GA could convert almost the entire incident solar light to heat energy. Solar steam generation efficiencies of 53.6 +/– 2.5% and 82.7 +/– 2.5% were achieved at light intensities of 1 and 10 kW/m^2, respectively [34].

1.3. Polymer composite materials

Synthetic polymer composites can reduce the materials cost of solar desalination. Polyurethane sponge is widely used in industry because of its micropore structures, excellent thermal insulation and scalable production. Wang et al. [35] introduced a novel photoreceiver composed of reduced graphene oxide (rGO) and polyurethane (PU) matrix for highly efficient solar steam generation. With excellent mechanical and chemical stability, the functional rGO/PU foam exhibited a solar photothermal efficiency of ~81% at a light density of 10 kW/m^2. Polydopamine and Cl-doped polypyrrole were successively modified onto the sand surface for a stable structure. Owing to the specific aggregative structure of the black sands, a self-channelled device combined adjustable 2D/3D solar-driven evaporation could be readily achieved, and yield a high evaporation performance (1.43 kg/m^2 h) [36]. Xu et al. [37] developed a flexible Janus solar absorber by sequential electrospinning which enabled a high efficiency of 72% and stable water output of 1.3 kg/m^2 h over 16 d under 1 sun.

1.4. Biological composite materials

Recent studies had reported a variety of artificial structures that are designed and fabricated to improve energy conversion efficiencies by enhancing solar absorption, heat localization, water supply, and vapor transportation. Mushrooms, as a kind of living organism, were surprisingly found to be efficient solar steam-generation devices for the first time [38]. Natural and carbonized mushrooms could achieve ≈62% and ≈78% conversion efficiencies under 1-sun illumination, respectively. With ultrahigh solar absorbance (~99%), low thermal conductivity (0.33 W/m K), and good hydrophilicity, the flame-treated wood could localize the solar heating at the evaporation surface and enable a solar-thermal efficiency of ~72% under 1-sun [39]. The use of carbon nanotube (CNT)-modified flexible wood membrane (F-Wood/CNTs) was demonstrated as a flexible, portable, recyclable, and efficient solar steam generation device for low-cost and scalable solar steam generation applications. The solar steam generation device based on the F-Wood/CNTs membrane exhibited a high efficiency of 81% at 10 kW/m^2 [40]. A novel bilayered structure comprised of wood and graphene oxide (GO) for highly efficient

solar steam generation was introduced [41]. The wood-GO composite structure exhibited a solar thermal efficiency of ~83% under simulated solar excitation at a power density of 12 kW/m^2.

Herein, a black nylon fiber flocking board with a vertically aligned array was prepared via a convenient electrostatic flocking technique. It presented an extremely high solar absorbance, a water self-supply capability, and a unique salt self-dissolution capability for seawater desalination. The evaporation test-bed was built, and the seawater evaporation performance evaluation and crystallization scaling tendency analysis were carried out through the experimental verification method. Finally, the freshwater production experiment of evaporation and condensation is carried out by simulating the traditional disc solar distiller.

2. Preparation and experimental system of photothermal conversion materials

2.1. Preparation of ultra-black nylon flocking photothermal conversion materials

As shown in Fig. 1, 0.6 mm long black nylon fiber was placed on the bottom plate of the high-voltage electrostatic device, and the paperboard was pasted on the top plate. A 100 μm thick acrylic adhesive layer was coated on the paperboard. The distance between the top and bottom plates was 100 mm. The voltage of the high-voltage electrostatic output machine was modulated to 40 kV, and the power was turned on for 5 s. By applying a potential of 40 kV between the two plates, the black nylon fibers became charged and were propelled toward the opposing electrode because of electrostatic force, thus the black nylon fibers were successfully aligned along the electric field lines between the two electrode plates and inserted into acrylic adhesive layer. Most of the black nylon fibers formed a micron scale array structure on the paperboard. Finally, the prepared material was treated under room temperature for 24 h to cure the acrylic adhesive.

High voltage electrostatic flocking is an effective method to prepare dense black nylon fiber vertical array structure. Although this array structure is not completely regular (Fig. 2), the array structure gives the material extremely high light absorption performance and unique wicking ability simultaneously.

2.2. Experiment system

As shown in Fig. 3, the ultra-black nylon flocking material was cut into a disc (diameter of 62 mm). A piece of sponge (thickness of 3 mm) with the same size was attached to the bottom of the ultra-black material for water transporting

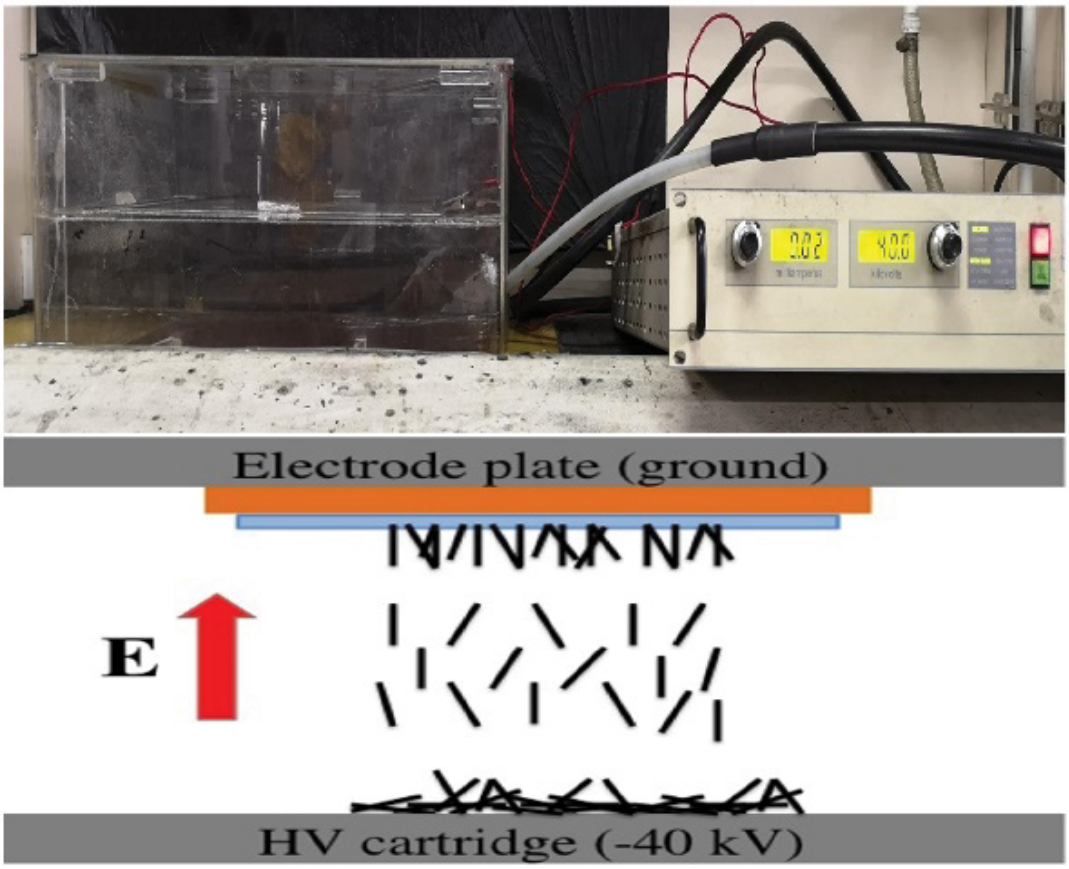

Fig. 1. Photo image and schematic of the electrostatic flocking device.

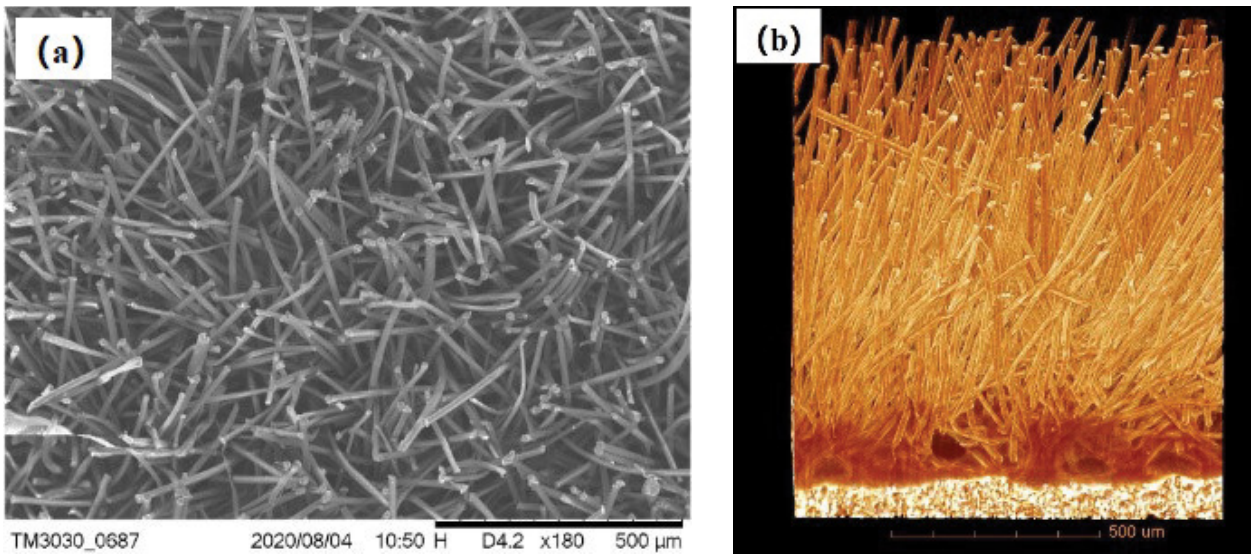

Fig. 2. (a) SEM image of the ultra-black nylon flocking material. (b) Micro CT image of the morphology of the ultra-black nylon flocking material.

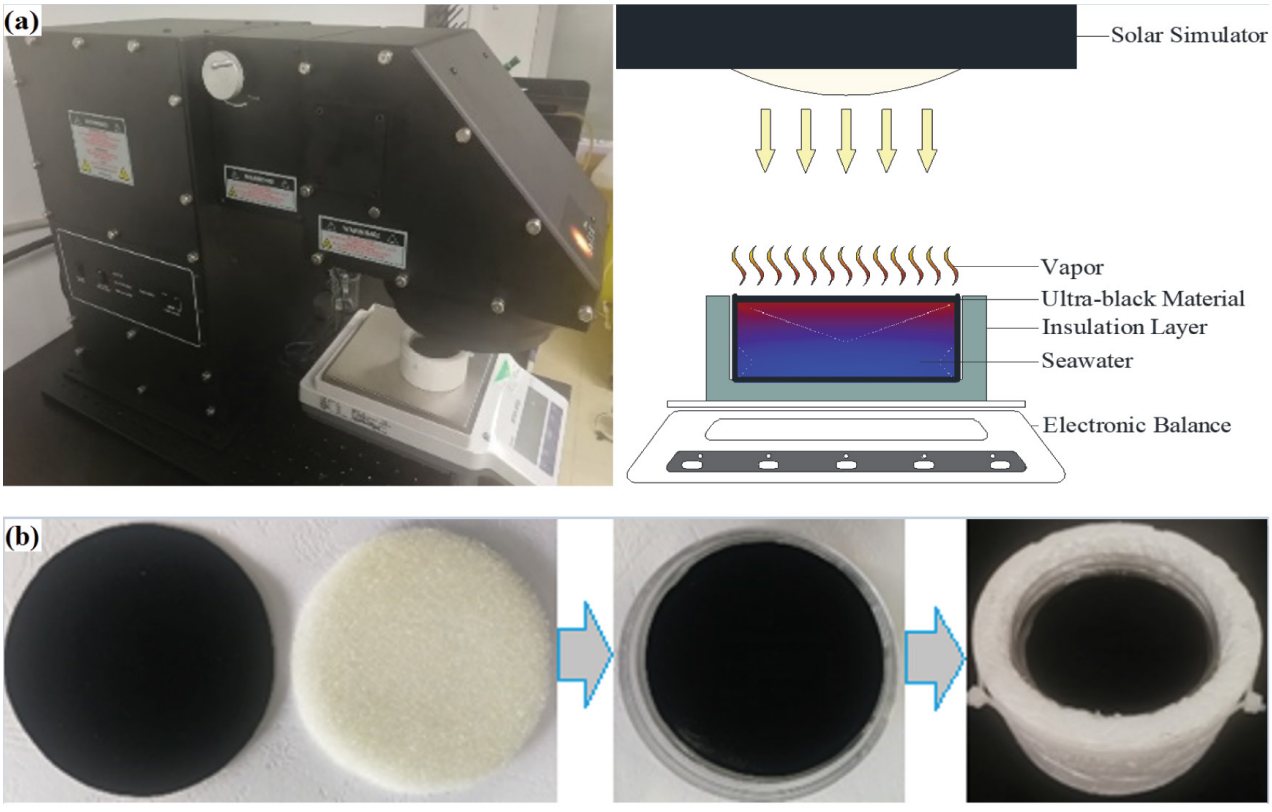

Fig. 3. (a) Photograph and schematic illustration of the setup of the seawater evaporation measurement with the ultra-black nylon flocking material floating on the seawater surface. (b) The preparation of the evaporating dish with the ultra-black nylon flocking material and the sponge.

and thermal insulation. Then the hybrid material was placed in an evaporating dish (inner diameter of 62 mm) and floated on the surface of the seawater in the evaporating dish. The surrounding and bottom of the evaporating dish were wrapped with polystyrene foam as the insulation layer. They were used as an evaporator and placed on a Mettler ME2002E electronic balance with a resolution of 0.01 g. The seawater mass reduction in the evaporator was recorded in real-time to calculate the steam generation rate and efficiency. The Newport94043A solar simulator

was used to simulate sunlight (Accuracy ±1 W/m^2), and its optical power density was calibrated with a 91,150 V reference battery for a standard sun, which was 1,000 W/m^2. During the experiment, the seawater temperature on the surface of the ultra-black nylon flocking material was tracked with a NEC TH7700 infrared thermal imaging camera (accuracy ±0.1°C), and the water temperature underneath the black material was measured with a Tondaj6801II high-precision digital thermometer (accuracy ±0.4°C). The uncertainty of the experiments had measured by the equations available in Essa et al. [42]. It had been found that the maximum uncertainty must not be increased by more than 2.3% during the experimentations.

3. Theoretical analysis

3.1. Bulk heating evaporation and interface heating evaporation

Traditional solar desalination uses solar radiation heat to heat seawater and increase the temperature of the bulk water. Since seawater has a very low absorption rate of sunlight, it cannot effectively absorb light energy for the evaporation of seawater. In order to improve the utilization efficiency of solar radiation heat energy, the researchers blackened the bottom of the sea pool, or added dyes, nanoparticles, etc. to the seawater. During the heating process of this bulk heating evaporation, a large amount of heat is used to heat and increase the temperature of the seawater, not only the steam generation efficiency is low, but also the heat loss is serious, and the overall seawater desalination efficiency is not high.

Compared with the bulk heating evaporation system, the interface heating evaporation system uses solar energy more efficiently in the process of steam generation (Fig. 4). This system is designed with light-absorbing materials to localize the heat energy on the surface of the material. The seawater on the surface of the material reaches a high temperature to facilitate the escape of steam. Therefore, the heat conduction loss to the water is reduced, and high light-thermal evaporation efficiency can be obtained at a lower light radiation intensity.

3.2. Solar absorbance of ultra-black nylon flocking material s

The solar radiation wavelength range covers the entire electromagnetic spectrum from X-ray to radio wave. About 99.9% of the energy in solar radiation is concentrated in 300–2,500 nm (ultraviolet, visible and near-infrared region) [43]. The absorbance of ultra-black nylon flocking material can reach 99.6% in the band range of 280–2,500 nm [44]. The excellent light absorption could be ascribed to the array structure of black nylon fiber, which constructs a good light trap, and limits the light reflection and scattering in the same time.

3.3. Seawater evaporation efficiency

The seawater evaporation efficiency was calculated based on the following equation.

$$\eta = \frac{\dot{m}\left(H_{LV} + Q\right)}{E_{in}} \quad (1)$$

where $\dot{m}$ refers to the evaporation rate, kg/m^2 h, H_{LV} refers to the total enthalpy that is required to cause the transition of seawater from its liquid to vapor phase $H_{LV}(T_e) = 1.91846 \times 10^6 \times [T_e/(T_e - 33.91)]^2$ (J/kg), T_e is the evaporation temperature measured experimentally (K); Q is the sensible heat of seawater per unit mass $Q = C_{cw} \times (T_e - T_0)$ (J/kg), where T_0 is the seawater temperature measured experimentally (K), C_{cw} is the seawater specific heat at the corresponding salinity and temperature $C_{cw} = A + Bt + Ct^2 + Dt^3$ (J/kg K), where t is the average temperature of seawater and evaporation temperature (°C), and the variables A, B, C and D are evaluated as a function of the water salinity as follows [45]:

$$A = 4{,}206.8 - 6.6197s + 1.2288 \times 10^{-2} \times s^2$$

$$B = -1.1262 + 5.4178 \times 10^{-2}s - 2.2719 \times 10^{-4}s^2$$

$$C = 1.2026 \times 10^{-2} - 5.3566 \times 10^{-4}s + 1.8906 \times 10^{-6}s^2$$

$$D = 6.8777 \times 10^{-7} + 1.517 \times 10^{-6}s - 4.4268 \times 10^{-9}s^2$$

where s is the salinity of seawater(g/kg); E_{in} refers to the total solar energy input per unit time on the system (kJ/m^2 h).

4. Results and discussion

The raw material seawater used in the experiment was taken from the Bohai Sea, and the conductivity of the seawater was 50.2 ms/cm. During all solar seawater evaporation experiments, the steam generation rate of 0.04 kg/m^2 h had been deducted under natural dark conditions to eliminate the influence of natural water evaporation [46]. All indoor experiments were conducted at room temperature of ~26°C and humidity of ~60%.

4.1. Seawater evaporation performance of the ultra-black nylon flocking materials

It can be seen from Fig. 5a that under 1 solar radiation intensity, the seawater temperature on the ultra-black nylon flocking photothermal conversion material surface is higher than that under the material. This is due to the thermal insulation effect of the material, which reduces the heat loss to the seawater under the material, and most of the heat is used for the evaporation of the surface seawater. Compared with the seawater temperature without this material, due to the light absorption performance of the material, both the surface temperature of the material and the bottom seawater temperature are highly increased.

It can be seen from Fig. 5b that the evaporation rate of seawater added with the ultra-black nylon flocking photothermal conversion material has been significantly improved. The average evaporation rate of seawater without this material is 0.71 kg/m^2 h, and the solar steam generation efficiency is 49.22%. After introducing the ultra-black nylon flocking photothermal conversion material, the average evaporation rate of seawater is 1.25 kg/m^2 h, the solar steam generation efficiency is 86.65%, and

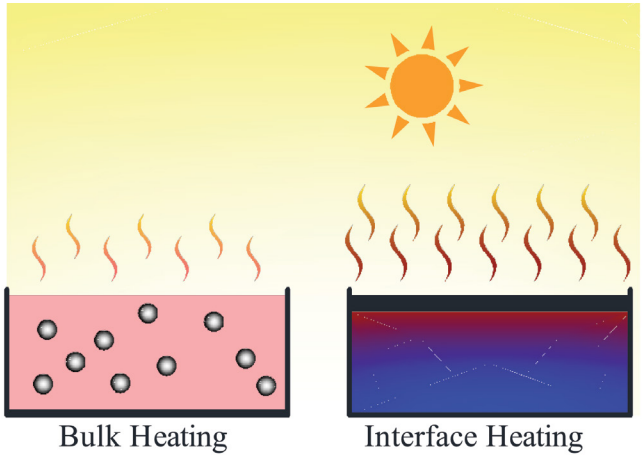

Fig. 4. Evaporation method of bulk heating and interface heating.

the evaporation performance is increased by 76.06%. The results show that the ultra-black nylon flocking material can significantly improve the evaporation performance of solar desalination.

4.2. Long-term operation stability analysis

The long-term stability of the photothermal conversion material is very important for practical applications. Good stability is conducive to the reuse of materials and cost saving, which is highly desired for large-scale industrial production of solar desalination. In the process of seawater desalination, the dissolved salts in seawater, such as sodium salt, calcium salt, magnesium salt, etc., will recrystallize under the influence of temperature and concentration. Under the driving force of capillary water absorption and evaporation, the seawater migrates to the top of nylon fiber and evaporates. After evaporation, the remaining seawater concentration is enriched. Due to the high evaporation rate, the dissolved salt may not have time to diffuse and dissolve in the water under the material and reach supersaturation, and crystalline salt may precipitate on the surface of the material. It can be seen from Fig. 6 that crystal salts begin to appear after 1 h of evaporation experiment. After 2 h of evaporation experiment, the formation of crystal salts is more obvious. After 8 h of solar radiation evaporation test, a large amount of crystal salts can be seen in the middle surface of the materials. This is because the capillary water absorption capacity of the material edge is greater than that of the middle part, which promotes the recrystallized salt after seawater evaporation to gather in the middle. At the end of the experiment as the solar simulator is turned off, the driving force of solar radiation evaporation is lost. The crystalline salt on the surface of the material dissolves rapidly at first, and then the dissolution rate slows down. This is because the gaps between the nylon fiber arrays act as dissolution and diffusion channels between the crystalline salt and the bottom seawater. After the self-dissolution process overnight, the crystallized salt on the surface of the material was completely dissolved. Scanning electron microscope (SEM) images of the materials before and after self-dissolution showed that the crystallized salts on the surface of nylon fiber had disappeared completely, and the original appearance was basically restored after self-dissolution.

For the experiment, the concentration ratio of seawater is less than 2. Solar radiation is alternating between day and night. After daily 8 h of solar radiation, the material floats still in sea water. When the experiment starts the next day, the crystalline salt has dissolved into the sea water by itself. After 20 repetitive experiments within a month, there are traces of insoluble salt on the surface of the material, and these crystalline salts cannot dissolve in seawater by themselves. It can be seen from Fig. 7 that the evaporation rate has slightly decreased, but the average evaporation rate is still stable above 1.20 kg/m^2 h. It shows that the insoluble crystalline salt does not significantly limit the seawater evaporation rate. Considering the influence of weather under natural conditions, the evaporation of

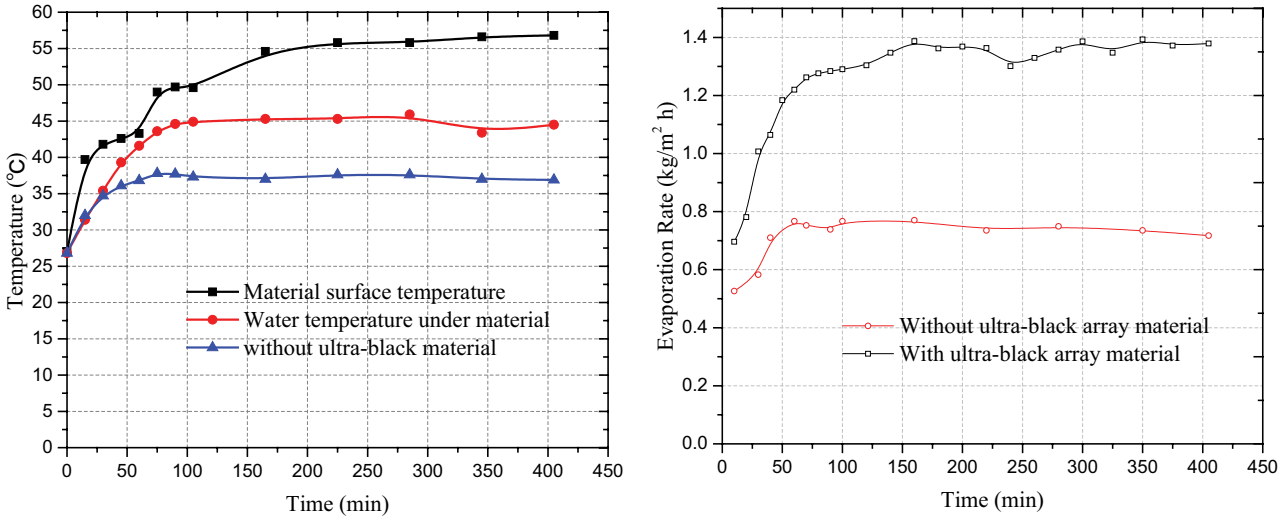

Fig. 5. (a) The temperatures changing of the seawater in the evaporating dish. (b) The evaporation rate under 1-sun illumination.

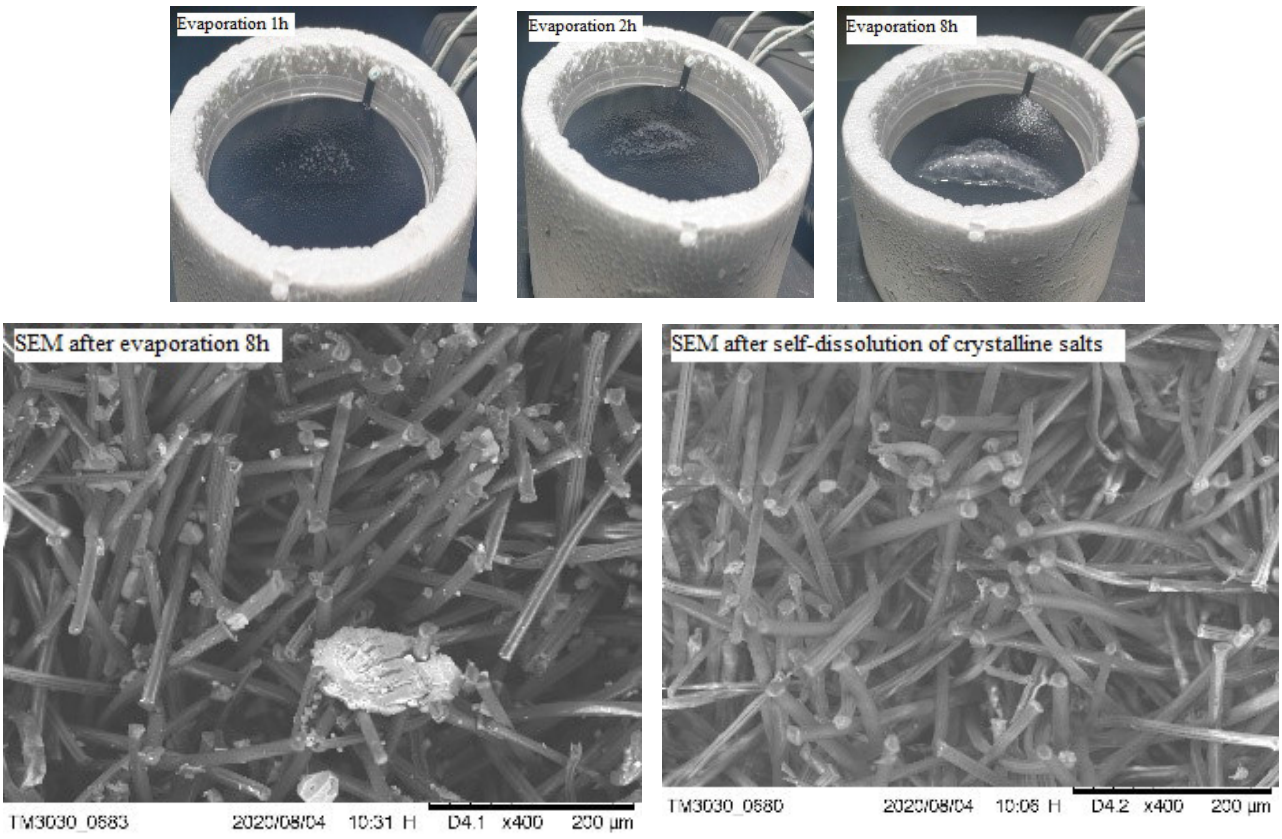

Fig. 6. Photographs of the ultra-black nylon flocking material in different time of solar seawater evaporation.

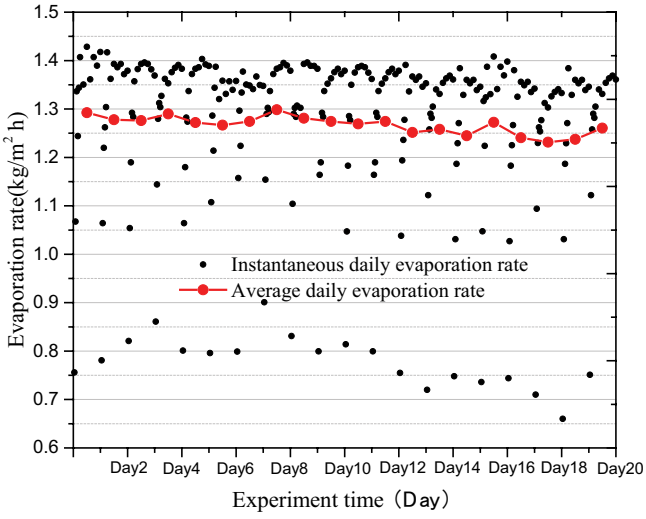

Fig. 7. Continuous experimental evaporation rate under one sun illumination.

seawater cannot reach the 24 h full-load operating condition per day. The reduction of evaporation intensity will provide greater self-dissolving ability of crystalline salt. Therefore, the ultra-black nylon flocking material has good long-term stability in the solar desalination process under natural conditions.

4.3. Evaporation and condensation experiment

Theoretical analysis and experiments have proved that the ultra-black nylon flocking photothermal conversion material can greatly improve the efficiency of solar seawater evaporation. But for the desalination process, what we ultimately need is fresh water, that is, to collect the evaporated steam, instead of dissipating the steam to the ambient environment. The solar distiller model with the simplest equipment and minimal investment is used for evaporation and condensation experiments. The steam evaporated in the solar distiller is condensed on the quartz glass cover (Fig. 8). The condensed water flows along the glass cover to the tray at the bottom of the distiller. There is a gap between the glass cover and the tray. The absorbent paper towels are used to suck the condensed water out from the gap. Because the distiller is placed on the electronic balance the real-time weight loss is tracked to indicate the real-time generation of vapor.

It can be seen from Fig. 9 that the evaporation rate of seawater with ultra-black nylon flocking material is significantly increased no matter whether the condensation cover is added or not, which indicates that the ultra-black nylon flocking material can improve the freshwater production in the actual seawater desalination process. Under the condition that the ultra-black nylon flocking material is installed, the evaporation rate of seawater without a condensation cover is higher than those with a condensation cover. This means that the steam

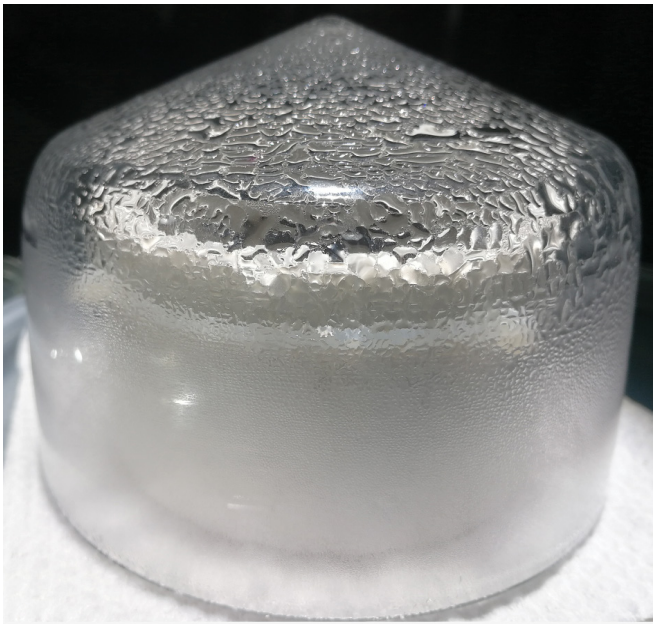

Fig. 8. Photo image of the seawater evaporation measurement with the condensing cover.

evaporated from sea water is not condensed on the condensing cover in time, which hinders the evaporation of seawater. Therefore, the actual solar desalination is necessary to enhance the condensation while improving the evaporation efficiency, such as increasing the emissivity of the condensation cover. The average evaporation rates of with ultra-black nylon flocking material without condensing cover, with ultra-black nylon flocking material with condensing cover and without ultra-black nylon flocking material with condensation cover were 1.28, 0.97 and 0.35 kg/m^2 h respectively. According to the effective sunshine time of 8 h/d, the freshwater production is 10.24, 7.76 and 2.8 kg/m^2 d respectively. This means that installing the ultra-black nylon flocking material in the traditional disc solar distiller can increase the freshwater production from the original 2.8–7.76 kg/m^2 d.

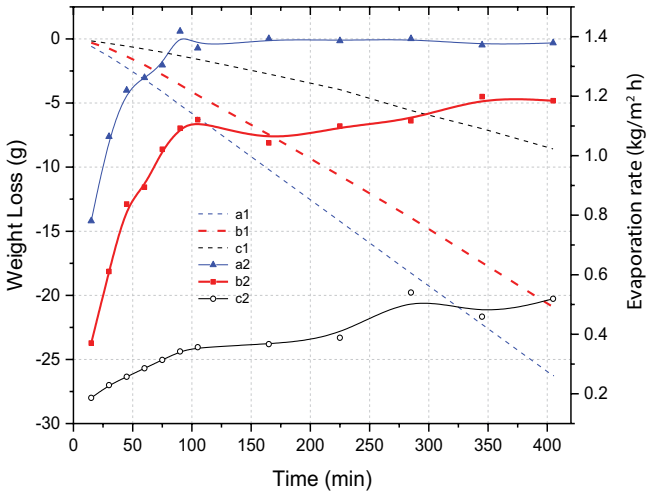

Fig. 9. Comparison of weight change and evaporation rates with or without condensing cover and the ultra-black nylon flocking material.

(a1) Weight loss without condensing cover and with ultra-black nylon flocking material; (b1) Weight loss with condensing cover and with ultra-black nylon flocking material; (c1) Weight loss with condensing cover and without ultra-black nylon flocking material; (a2) Evaporation rate without condensing cover and with ultra-black nylon flocking material; (b2) Evaporation rate with condensing cover and with ultra-black nylon flocking material; (c2) Evaporation rate with condensing cover and without ultra-black nylon flocking material;

5. Conclusions

The following conclusions are drawn:

- Electrostatic flocking is a cost-effective processing method and has been widely used in industrial applications. Utilizing such technology, an ultra-black nylon flocking photothermal conversion material has been developed. This material has a very high light absorption rate (99.6%) and special capillary water absorption performance due to the vertical fiber array structure. Tests have proved that with the addition of this material, the solar-driven seawater evaporation rate achieves 1.25 kg/m^2 h, and the long-term stability is demonstrated due to its salt self-dissolution capability.
- The evaporation and condensation experiments of the solar distiller have been carried out under a simulated sunlight source. The solar stiller is closer to practical industrial application. Compared with the traditional disc distiller without setting this ultra-black nylon flocking photothermal conversion materials, the water yield of this solar distiller increases from the original 2.8 to 7.76 kg/m^2 d. Without the cover of a closed condensation system, the vapor generation rate is 10.24 kg/m^2 d. It implies that promoting the condensation efficiency is possible to enhance the evaporation efficiency and water production performance for the solar desalination

system. Strategies to enhance the steam condensation efficiency is underway in our future work.

Acknowledgements

This work was jointly supported by the Science and Technology Program of Tianjin, China (grant no. 18YFYSZ C00060), and the National Key Research and Development Program of China (2018YFC0408002).

References

[1] M.A. Eltawil, Z. Zhengming, L. Yuan, A review of renewable energy technologies integrated with desalination systems, Renewable Sustainable Energy Rev., 13 (2009) 2245–2262.
[2] S. Kalogirou, Seawater desalination using renewable energy sources, Progr. Energy Combust. Sci., 31 (2005) 242–281.
[3] G.C. Pandey, Effect of dye on the performance of a double basin solar still, Int. J. Energy Res., 7 (1983) 327–332.
[4] C.E. Okeke, S.U. Egarievwe, A.O.E. Animalu, Effects of coal and charcoal on solar-still performance, Energy, 15 (1990) 1071–1073.
[5] S.W. Sharshir, A.H. Elsheikh, E.M.A. Edreis, M.K.A. Ali, R. Sathyamurthyi, A.E. Kabeel, J. Zang, N. Yang, Improving the solar still performance by using thermal energy storage materials: a review of recent developments, Desal. Water Treat., 165 (2019) 1–15.
[6] H.N. Panchal, P.K. Shah, Enhancement of upper basin distillate output by attachment of vacuum tubes with double-basin solar still, Desal. Water Treat., 55 (2014) 587–595.
[7] H. Panchal, H. Nurdiyanto, K.K. Sadasivuni, S.S. Hishan, F.A. Essa, M. Khalid, S. Dharaskar, S. Shanmugan, Experimental investigation on the yield of solar still using manganese oxide nanoparticles coated absorber, Case Stud. Therm. Eng., 25 (2021) 100905, doi: 10.1016/j.csite.2021.100905.
[8] A.M. Gandhi, S. Shanmugan, S. Gorjian, C.I. Pruncu, S. Sivakumar, A.H. Elsheikh, F.A. Essa, Z.M. Omara, H. Panchal, Performance enhancement of stepped basin solar still based on OSELM with traversal tree for higher energy adaptive control, Desalination, 502 (2021) 114926, doi: 10.1016/j.desal.2020.114926.
[9] P. Thamizharasu, S. Shanmugan, S. Gorjian, C.I. Pruncu, F.A. Essa, H. Panchal, M. Harish, Improvement of thermal performance of a solar box type cooker using SiO_2/TiO_2 nanolayer, Silicon, (2020), doi: 10.1007/s12633-020-00835-1.
[10] A.S. Abdullah, Z.M. Omara, F.A. Essa, M.M. Younes, S. Shanmugan, M. Abdelgaied, M.I. Amro, A.E. Kabeel, W.M. Farouk, Improving the performance of trays solar still using wick corrugated absorber, nano-enhanced phase change material and photovoltaics-powered heaters, J. Energy Storage, 40 (2021) 102782, doi: 10.1016/j.est.2021.102782.
[11] F.A. Essa, Z. Omara, A. Abdullah, S. Shanmugan, H. Panchal, A.E. Kabeel, R. Sathyamurthy, M.M. Athikesavan, A. Elsheikh, M. Abdelgaied, B. Saleh, Augmenting the productivity of stepped distiller by corrugated and curved liners, CuO/paraffin wax, wick, and vapor suctioning, Environ. Sci. Pollut. Res. Int., 28 (2021) 56955–56965.
[12] M.M. Younes, A.S. Abdullah, F.A. Essa, Z.M. Omara, M.I. Amro, Enhancing the wick solar still performance using half barrel and corrugated absorbers, Process Saf. Environ. Prot., 150 (2021) 440–452.
[13] A.S. Abdullah, F.A. Essa, H.B. Bacha, Z.M. Omara, Improving the trays solar still performance using reflectors and phase change material with nanoparticles, J. Energy Storage, 31 (2020) 101744, doi: 10.1016/j.est.2020.101744.
[14] M.M. Thalib, A.M. Manokar, F.A. Essa, N. Vasimalai, R. Sathyamurthy, F.P. Garcia Marquez, Comparative study of tubular solar stills with phase change material and nano-enhanced phase change material, Energies, 13 (2020) 3989, doi: 10.3390/en13153989.
[15] A.E. Kabeel, R. Sathyamurthy, A.M. Manokar, S.W. Sharshir, F.A. Essa, A.H. Elshiekh, Experimental study on tubular solar still using graphene oxide nano particles in phase change material (NPCM's) for fresh water production, J. Energy Storage, 28 (2020) 101204, doi: 10.1016/j.est.2020.101204.
[16] Z. Chen, J. Peng, G. Chen, L. Hou, T. Yu, Y. Yao, H. Zheng, Analysis of heat and mass transferring mechanism of multi-stage stacked-tray solar seawater desalination still and experimental research on its performance, Solar Energy, 142 (2017) 278–287.
[17] B.H. Upadhyay, A.J. Patel, K.K. Sadasivuni, J.M. Mistry, P.V. Ramana, H. Panchal, D. Ponnamma, F.A. Essa, Design, development and techno economic analysis of novel parabolic trough collector for low-temperature water heating applications, Case Stud. Therm. Eng., 26 (2021) 100978, doi: 10.1016/j.csite.2021.100978.
[18] M. Abd Elaziz, F.A. Essa, A.H. Elsheikh, Utilization of ensemble random vector functional link network for freshwater prediction of active solar stills with nanoparticles, Sustainable Energy Technol. Assess., 47 (2021) 101405, doi: 10.1016/j.seta.2021.101405.
[19] F.A. Essa, F.S. Abou-Taleb, M.R. Diab, Experimental investigation of vertical solar still with rotating discs, Energy Sources Part A, (2021) 1–21, doi: 10.1080/15567036.2021.1950238.
[20] W.H. Alawee, S.A. Mohammed, H.A. Dhahad, A.S. Abdullah, Z.M. Omara, F.A. Essa, Improving the performance of pyramid solar still using rotating four cylinders and three electric heaters, Process Saf. Environ. Prot., 148 (2021) 950–958.
[21] Z.M. Omara, A.S. Abdullah, F.A. Essa, M.M. Younes, Performance evaluation of a vertical rotating wick solar still, Process Saf. Environ. Prot., 148 (2021) 796–804.
[22] A.S. Abdullah, Z.M. Omara, F.A. Essa, A. Alarjani, I.B. Mansir, M.I. Amro, Enhancing the solar still performance using reflectors and sliding-wick belt, Sol. Energy, 214 (2021) 268–279.
[23] F.A. Essa, A.S. Abdullah, Z.M. Omara, Improving the performance of tubular solar still using rotating drum – experimental and theoretical investigation, Process Saf. Environ. Prot., 148 (2021) 579–589.
[24] A.S. Abdullah, A. Alarjani, M.M. Abou Al-Sood, Z.M. Omara, A.E. Kabeel, F.A. Essa, Rotating-wick solar still with mended evaporation technics: experimental approach, Alexandria Eng. J., 58 (2019) 1449–1459.
[25] F.A. Essa, W.H. Alawee, S.A. Mohammed, A.S. Abdullah, Z.M. Omara, Enhancement of pyramid solar distiller performance using reflectors, cooling cycle, and dangled cords of wicks, Desalination, 506 (2021) 115019, doi: 10.1016/j.desal.2021.115019.
[26] F.A. Essa, Z.M. Omara, A.S. Abdullah, S. Shanmugan, H. Panchal, A.E. Kabeel, R. Sathyamurthy, W.H. Alawee, A.M. Manokar, A.H. Elsheikh, Wall-suspended trays inside stepped distiller with Al_2O_3/paraffin wax mixture and vapor suction: experimental implementation, J. Energy Storage, 32 (2020) 102008, doi: 10.1016/j.est.2020.102008.
[27] F.A. Essa, A.S. Abdullah, Z.M. Omara, A.E. Kabeel, Y. Gamiel, Experimental study on the performance of trays solar still with cracks and reflectors, Appl. Therm. Eng., 188 (2021) 116652, doi: 10.1016/j.applthermaleng.2021.116652.
[28] K. Bae, G. Kang, S.K. Cho, W. Park, K. Kim, W.J. Padilla, Flexible thin-film black gold membranes with ultrabroadband plasmonic nanofocusing for efficient solar vapour generation, Nat. Commun., 6 (2015) 10103, doi: 10.1038/ncomms10103.
[29] L. Zhou, Y. Tan, J. Wang, W. Xu, Y. Yuan, W. Cai, S. Zhu, J. Zhu, 3D self-assembly of aluminium nanoparticles for plasmon-enhanced solar desalination, Nat. Photonics, 10 (2016) 393–398.
[30] H. Ghasemi, G. Ni, A.M. Marconnet, J. Loomis, S. Yerci, N. Miljkovic, G. Chen, Solar steam generation by heat localization, Nat. Commun., 5 (2014) 4449, doi: 10.1038/ncomms5449.
[31] Y. Yang, R. Zhao, T. Zhang, K. Zhao, P. Xiao, Y. Ma, P.M. Ajayan, G. Shi, Y. Chen, Graphene-based standalone solar energy converter for water desalination and purification, ACS Nano, 12 (2018) 829–835.
[32] H. Ren, M. Tang, B. Guan, K. Wang, J. Yang, F. Wang, M. Wang, J. Shan, Z. Chen, D. Wei, H. Peng, Z. Liu, Hierarchical graphene foam for efficient omnidirectional solar–thermal energy

conversion, Adv. Mater., 29 (2017) 1702590, doi: 10.1002/adma.201702590.
[33] Z. Liu, H. Song, D. Ji, C. Li, A. Cheney, Y. Liu, N. Zhang, X. Zeng, B. Chen, J. Gao, Y. Li, X. Liu, D. Aga, S. Jiang, Z. Yu, Q. Gan, Extremely cost-effective and efficient solar vapor generation under nonconcentrated illumination using thermally isolated black paper, Global Challenges, 1 (2017) 1600003, doi: 10.1002/gch2.201600003.
[34] Y. Fu, G. Wang, T. Mei, J. Li, J. Wang, X. Wang, Accessible graphene aerogel for efficiently harvesting solar energy, ACS Sustainable Chem. Eng., 5 (2017) 4665–4671.
[35] G. Wang, Y. Fu, A. Guo, T. Mei, J. Wang, J. Li, X. Wang, Reduced graphene oxide–polyurethane nanocomposite foam as a reusable photoreceiver for efficient solar steam generation, Chem. Mater., 29 (2017) 5629–5635.
[36] F. Ni, P. Xiao, N. Qiu, C. Zhang, Y. Liang, J. Gu, J. Xia, Z. Zeng, L. Wang, Q. Xue, T. Chen, Collective behaviors mediated multifunctional black sand aggregate towards environmentally adaptive solar-to-thermal purified water harvesting, Nano Energy, 68 (2020) 104311, doi: 10.1016/j.nanoen.2019.104311.
[37] W. Xu, X. Hu, S. Zhuang, Y. Wang, X. Li, L. Zhou, S. Zhu, J. Zhu, Flexible and salt resistant janus absorbers by electrospinning for stable and efficient solar desalination, Adv. Energy Mater., 8 (2018) 1702884, doi: 10.1002/aenm.201702884.
[38] N. Xu, X. Hu, W. Xu, X. Li, L. Zhou, S. Zhu, J. Zhu, Mushrooms as efficient solar steam-generation devices, Adv. Mater., 29 (2017) 1606762, doi: 10.1002/adma.201606762.
[39] G. Xue, K. Liu, Q. Chen, P. Yang, J. Li, T. Ding, J. Duan, B. Qi, J. Zhou, Robust and low-cost flame-treated wood for high-performance solar steam generation, ACS Appl. Mater. Interfaces, 9 (2017) 15052–15057.
[40] C. Chen, Y. Li, J. Song, Z. Yang, Y. Kuang, E. Hitz, C. Jia, A. Gong, F. Jiang, J.Y. Zhu, B. Yang, J. Xie, L. Hu, Highly flexible and efficient solar steam generation device, Adv. Mater., 29 (2017) 1701756, doi: 10.1002/adma.201701756.
[41] K.K. Liu, Q. Jiang, S. Tadepalli, R. Raliya, P. Biswas, R.R. Naik, S. Singamaneni, Wood-graphene oxide composite for highly efficient solar steam generation and desalination, ACS Appl. Mater. Interfaces, 9 (2017) 7675–7681.
[42] F.A. Essa, Z.M. Omara, A.S. Abdullah, A.E. Kabeel, G.B. Abdelaziz, Enhancing the solar still performance via rotating wick belt and quantum dots nanofluid, Case Stud. Therm. Eng., 27 (2021) 101222, doi: 10.1016/j.csite.2021.101222.
[43] R.-C. Juang, Y.-C. Yeh, B.-H. Chang, W.-C. Chen, T.-W. Chung, Preparation of solar selective absorbing coatings by magnetron sputtering from a single stainless steel target, Thin Solid Films, 518 (2010) 5501–5504.
[44] C. Tu, W. Cai, X. Chen, X. Ouyang, H. Zhang, Z. Zhang, A 3D-structured sustainable solar-driven steam generator using super-black nylon flocking materials, Small, 15 (2019) e1902070, doi: 10.1002/smll.201902070.
[45] H.T. El-Dessouky, H.M. Ettouney, Fundamentals of Salt Water Desalination, Elsevier, Amsterdam, 2002.
[46] M.Z.W.Z.W.D.H. Zhu, Preparation and solar water evaporation performance of Ag@Ag_2S/C photothermal conversion materials, J. Qingdao Univ. Sci. Technol. (Nat. Sci. Ed.), 40 (2019) 69–74.